



computational proteomics

Laboratory for Computational Proteomics

www.FenyoLab.org

E-mail: Info@FenyoLab.org

Facebook: [NYUMC Computational Proteomics Laboratory](#)

Twitter: [@CompProteomics](#)

MeV ion sputtering of polymers: correlation between secondary ion radial velocity distributions and heavy ion track structure

R.M. Papaléo ^{*1}, G. Brinkmalm, D. Fenyő, J. Eriksson, H.-F. Kammer, P. Demirev, P. Håkansson and B.U.R. Sundqvist

Division of Ion Physics, Department of Radiation Sciences, Uppsala University, Box 535, 751 21 Uppsala, Sweden

Systematic investigations of the initial radial velocity distributions of low mass positive and negative secondary ions, sputtered electronically from thin films of polyvinylidene fluoride and polystyrene, are reported. 72.3 MeV $^{127}\text{I}^{13+}$ primary ions bombard the targets at 45° angle of incidence. Sputtered secondary ions in an individual MeV ion impact are analysed in a high resolution time-of-flight mass spectrometer. The accurate mass measurements of all ion peaks in the range from 1 to 100 m/z provide unequivocal determination of the chemical composition of these ions, forming homologous series, C_nH_m^\pm and $\text{C}_n\text{H}_m\text{F}_p^\pm$. Plots of both the initial mean radial velocity ($\langle v_x \rangle$) and kinetic energy ($\propto \langle v_x^2 \rangle$) as a function of the ion m/z results in a periodic pattern. Ions with lower hydrogen content exhibit wider velocity distributions (i.e. higher $\langle v_x^2 \rangle$) and $\langle v_x \rangle$ directed towards the primary ion trajectory. Ions with higher hydrogen content have lower mean kinetic energies and $\langle v_x \rangle$ directed away from the incident ion trajectory. We argue that the $\langle v_x \rangle$ and $\langle v_x^2 \rangle$ periodic behaviour, connected to the chemical constitution of the ions, reflects the radial profile of the deposited energy density in the heavy ion track.

1. Introduction

The production of damage tracks [1,2] is one among a number of notable effects of the interaction of swift heavy ions with dielectric materials. Two other effects include incident ion-induced nonequilibrium chemistry in solids [3,4], resulting in radiation damage, and sputtering processes [5], causing material erosion. Interconnections among all these phenomena were discussed and demonstrated long ago [6]. For instance, Haff [7] proposed a model for energy deposition in an insulator, linking both track formation and sputtering to the electronic part of the excitation caused by the MeV heavy ion. The properties of latent nuclear tracks have been monitored *ex situ* by a plethora of physical methods [2,8]. On the other hand, studies of properties of ions, sputtered electronically in a single MeV heavy ion impact, may provide direct *in situ* information for the complex physical and chemical processes leading to track formation, as has been argued recently [9,10].

The mechanisms of the electronic sputtering phenomenon have been studied quite extensively [11,12]. Experimental results [13,14] and theoretical calculations provide strong indications that high mass molecular ions (e.g. peptide ions) are ejected from the ultratrack by a transient energy flow (pressure pulse [15] or

shock wave [16]) propagating radially from the track core. This is observed as an off normal maximum in the radial velocity distribution. On the other hand, low mass fragment ions like CH_3^+ and C_2H_3^+ are emitted preferentially normal to the target surface [17]. They have an initial radial velocity distribution symmetric around the surface normal as expected for ions ejected in a thermal evaporation type process. It has been assumed a priori that all the other low mass fragment ions present in the secondary ion mass spectra, would also follow the behaviour observed for CH_3^+ and few other low mass ions. Data on the velocity distribution of more than 200 different positive and negative low mass ions (m/z below 100) ejected from polymeric films are presented in this paper. We have observed that the positive ions do not show a homogeneous behaviour. The characteristics of the radial velocity distributions (i.e. the mean velocity ($\langle v_x \rangle$) and the width ($\propto \langle v_x^2 \rangle$)) depend on the chemical composition or, more specifically, on the degree of hydrogenation of the secondary ions. Moreover, we argue that information derived from the $\langle v_x \rangle$ and $\langle v_x^2 \rangle$ of these ions allows us to probe, *in situ*, events in the MeV ion track during the early stages of its creation.

2. Experimental

72.3-MeV $^{127}\text{I}^{13+}$ ions from the Uppsala EN-tandem accelerator, incident on the target at an angle of 45°, were used as projectiles. The target was held at an

* Corresponding author.

¹ Fellow from the Institute of Physics, Federal University of Rio Grande do Sul, Porto Alegre, Brazil.

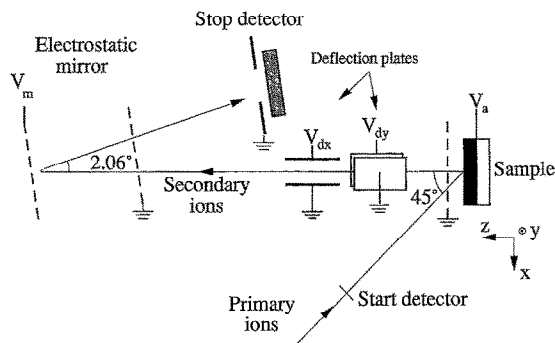


Fig. 1. Experimental set-up for the radial velocity measurements. The primary ion trajectory lies in the xz plane. For further details see ref. [19].

extraction potential V_a of ± 14.30 kV for positive and negative secondary ions respectively. The ejected secondary ions were analysed in a reflectron TOF mass spectrometer [18], with the electrostatic ion mirror maintained at a potential $V_m + (-)15.66$ kV for positive (negative) secondary ions. The ion flight time registration was performed in a pulse counting mode by employing a time-to-digital converter (IPN, Orsay, France) with 0.5 ns time resolution. Data were acquired in an event-by-event mode, at a rate of 2×10^3 incident MeV ions per second. The targets were prepared by spin-coating PVDF ($[-\text{CH}_2\text{CF}_2-]_n$, Aldrich Chemical Co.) and PS ($[-\text{CH}_2\text{CH}(\text{C}_6\text{H}_5)-]_n$, BASF) thin films (between 500 and 1000 Å) on silicon substrates.

The procedure for the measurement of the initial radial (tangential) velocity distribution has been described in more detail in refs. [17,19]. Throughout the paper we have used the term “radial velocity” for brevity, although its x -component, v_x , see Fig. 1, was actually measured and reported. The measurements involved monitoring the secondary ion yield as a function of the electrostatic deflection in the x - or y -direction perpendicular to the target surface normal. To determine v_x , the yield of low mass ions was maximised by setting the appropriate potential on the y -deflection plates, and then acquiring data for different voltages V_{dx} applied to the x -deflection plates. Conversion from deflection voltage units to velocity units for different ions was performed according to [17,19]:

$$v_x = k_x \frac{V_{dx} - V_{0d}}{\sqrt{m}}, \quad (1)$$

where m and q are the ion mass and charge and k_x is a constant depending on V_a , V_m and on the geometrical parameters of the instrument [19]. V_{0d} in Eq. (1) is the voltage on the deflection plates required for an ion with zero radial velocity to reach the centre of the stop detector. For a perfect alignment between the spec-

trometer optical axis, the beam spot position and the normal to the sample surface, $V_{0d} = 0$. This condition is very difficult to achieve and the centroids of the velocity distribution of C_2H_3^+ ions, shown previously to be ejected preferentially normal to the target surface ($\langle v_x \rangle = 0$) [17], was used for estimating V_{0d} . For the negative ions, V_{0d} was determined from the centroid of the C_2H_2^- velocity distribution. The velocity distributions were obtained by fitting the experimental data to a Gaussian curve. The quantities of interest: the mean radial velocities $\langle v_x \rangle$, and the mean square velocities, $\langle v_x^2 \rangle$, were calculated using Eq. (1) and averaging over the velocity distributions for each ion.

3. Results and discussion

The first step in this investigation has been to establish a reliable correspondence between a mass line in the secondary ion spectrum and the chemical composition of the ion associated with this mass. This is not straightforward particularly in the spectra from PVDF samples. The presence of three different chemical elements (C, H, F) in PVDF yields sometimes more than one possible chemical composition for a given integer mass. The use of a high resolution time-of-flight mass spectrometer has allowed separation of peaks, corresponding to ions with same integer m/z that differ at least by ≈ 0.02 u (in the $m/z < 100$ region). The mass accuracy, Δm , defined as the difference between the measured mass of a certain ion and the expected mass (calculated from the proposed chemical composition of this ion) has been, on the average, 0.004 u. This accuracy has been sufficient to obtain an unequivocal determination of the chemical composition for most of the secondary ions. When Δm approached 0.01 u the tentative chemical assignment has been considered inadequate. Based on this method of peak identification, it has been concluded that the low mass ions ejected from PVDF form two homologous series, C_nH_m^\pm and $\text{C}_n\text{H}_m\text{F}^\pm$ ($n = 1$ to 8, $m = 0$ to $2n + 1$), plus several ions with 2 or 3 F atoms. In the case of PS, hydrocarbon ions, C_nH_m^\pm , dominate the whole mass spectrum as expected. Breaking and rearrangement of the polymer backbone, and reactions involving hydrogen, lead to ions with the mentioned chemical composition. A contribution to the secondary ion yields from contaminants present on the sample surface could not be excluded. Possible mechanisms of C–H bond breaking, initiated by a heavy MeV ion impact, have already been discussed [20].

A plot of $\langle v_x \rangle$ as a function of the positive secondary ion m/z results in an “oscillating” behaviour (Figs. 2 and 3). This behaviour is related to the chemical constitution homology of the ions, with 12 (one C atom) as a repeat unit. The v_x velocity distributions

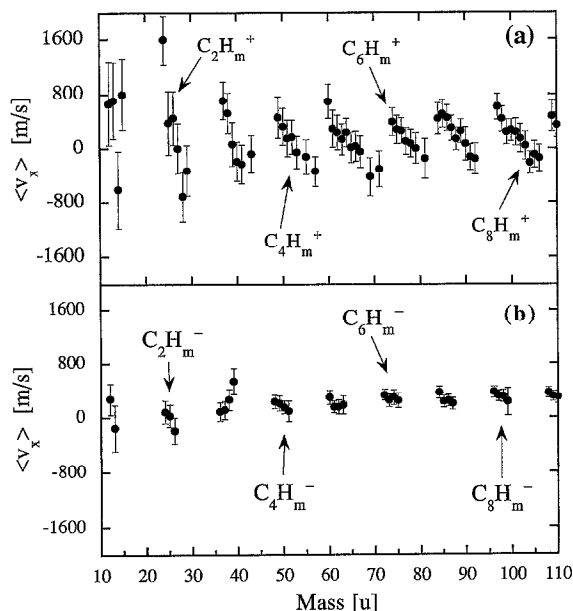


Fig. 2. Mean radial velocities $\langle v_x \rangle$ for the $C_nH_m^+$ (a) and $C_nH_m^-$ (b) ion series from polystyrene as a function of ion mass.

are not peaked around the normal to the surface, that is $\langle v_x \rangle \neq 0$, for most of the low mass positive ions from both PVDF and PS. It is clearly seen from Figs. 2a and Fig. 3 that ions with no hydrogen or low hydrogen content have velocities with positive sign (ejected away

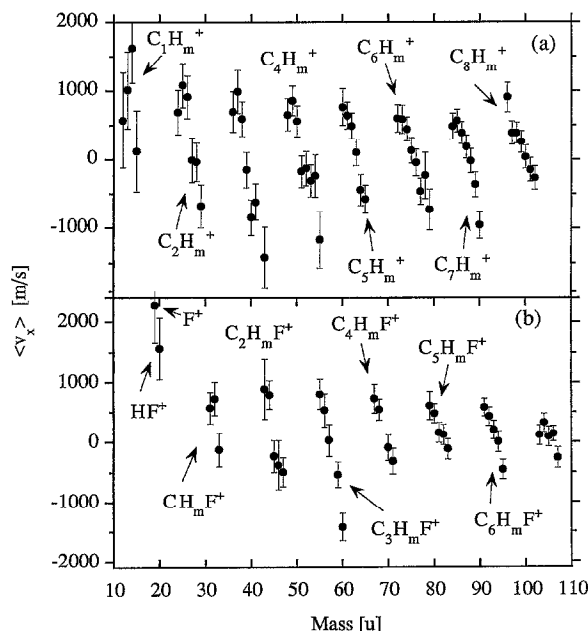


Fig. 3. Mean radial velocities $\langle v_x \rangle$ for (a) the $C_nH_m^+$ ion series and (b) $C_nH_mF^+$ ion series ejected from PVDF as a function of ion mass.

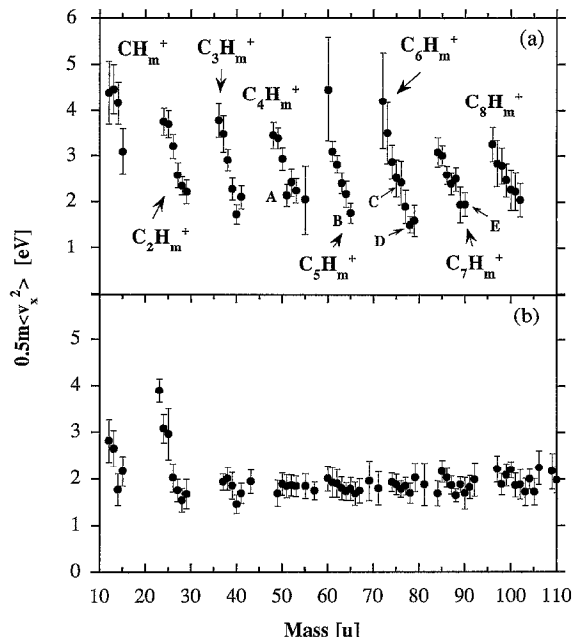


Fig. 4. Radial kinetic energy ($\langle E_x \rangle = 0.5m\langle v_x^2 \rangle$) of ions ejected from (a) PVDF and (b) PS, as a function of ion mass. The capital letters beside some experimental points indicate the ions for which the C_nH_m assignment is not evident. The possible chemical composition of these ions are: A: CF_2H^+ and $C_4H_3^+$; B: $C_2F_2H_3^+$ and $C_5H_5^+$; C: $C_3F_2H^+$ and $C_6H_3^+$; D: $C_3F_2H_3^+$ and $C_6H_5^+$; E: $C_4F_2H_4^+$ and $C_7H_6^+$.

from the surface normal, and *towards* the primary ion trajectory, Fig. 1). The values of $\langle v_x \rangle$ decrease for ions with higher hydrogen content reaching eventually negative sign for ions with the highest number of hydrogen atoms in each $C_nH_m^+$ or $C_nH_mF^+$ series. These ions are ejected again off the surface normal, but *away* from the incident ion trajectory. In other words, the degree of hydrogenation (m/n) for different positive ion series is correlated to the sign of $\langle v_x \rangle$. A difference between $\langle v_x \rangle$ for $C_2H_3^+$ and for the other low mass ions is clearly seen. This “shift” is similar to the one observed for large biomolecules [13,14], and indicates in analogy that a non-random momentum transfer is also involved in the sputtering of the low mass species. In a striking contrast to the positive ions, the negative $C_nH_m^-$ ions from both PVDF and PS have $\langle v_x \rangle$ that are constant (Fig. 2b).

The plot of $\langle E_x \rangle$ ($= 0.5m\langle v_x^2 \rangle$, linked to the FWHM of the v_x -velocity distribution) versus mass of positive ions ejected from PVDF and PS is given on Fig. 4. For ions ejected from PVDF there exists a correlation between $\langle E_x \rangle$ and chemical composition: ions with higher degree of hydrogenation have lower mean radial kinetic energies and vice versa. Most ions from PS targets, on the contrary, exhibit a much weaker dependence of $\langle E_x \rangle$ on ion mass, compared to PVDF.

We stress that the $\langle v_x \rangle$ and $\langle E_x \rangle$ obtained here should not be considered as absolute values for the radial velocity and for the associated kinetic energy of the secondary ions. As mentioned previously, the zero of the velocity axis is defined through the centroid of the $C_2H_3^+$ v_x -distribution. Although such a choice is based on experimental evidence [14,17] it still introduces an uncertainty in the scaling of the $\langle v_x \rangle$. Moreover, the $\langle E_x \rangle$ values are an upper limit to the values of the secondary ion mean radial energies. Factors like the finite size of the stop detector [17] and the diverging effect of the acceleration grid [21] also contribute to the broadening of the velocity distributions and hence to the calculated value of $\langle E_x \rangle$. Nonetheless, these contributions do not influence the relative values of $\langle v_x \rangle$ and $\langle E_x \rangle$ between different secondary ions, which is the most important information in the context of this work.

It is well known that the energy deposited in a heavy ion track is not restricted to the direct transfer of energy from the ion to the target atoms in its path through the solid. There is also a lateral spread of the deposited energy due to e.g. the energetic secondary electrons produced in the primary ionizations [22] and a transient pressurized disturbance originating from the large energy gradient close to the ion track [15]. Most of the deposited energy ($\approx 80\%$) is confined within the infratrack [23]. A rough estimation of the energy density deposited within the infratrack of a 72.3 MeV $^{127}I^{13+}$ ion in PVDF gives a figure of ≈ 20 eV/Å³. The volume occupied by each PVDF repeating unit is approximately 30 Å³, meaning that each PVDF monomer in the infratrack receives ≈ 600 eV. Similar values are obtained for PS. Thus a complete destruction of the polymer chains together with the preferential elimination (by diffusion and/or ejection) of H and F atoms, occurs in the inner-most parts of the track where the energy density is highest. Pure carbon clusters C_n^+ , which have the broadest velocity distributions (or the highest $\langle E_x \rangle$) should originate preferentially from this “hot” region. The lower $\langle E_x \rangle$ of ions with increasing number of hydrogen atoms indicates that they are formed farther away from the track core where the energy density is lower. At this region the survival probability for hydrogenated fragments increases, and recombination reactions of H and F with C-atoms can also be more probable. The decrease in the width (mean kinetic energy) of the velocity distributions with increase in the hydrogen content reflects the radial profile of the deposited energy density in the heavy ion track.

The variation of the $\langle v_x^2 \rangle$ with degree of hydrogenation of the $C_nH_m^+$ ions vanishes after the $C_2H_m^+$ series in PS (Fig 4b). A weak dependence of the $\langle v_x^2 \rangle$ on the hydrogen content can be discerned in some of the higher $C_nH_m^+$ series (e.g. $C_5H_m^+$ and $C_7H_m^+$), but the

small variations are on the order of our experimental uncertainties. The lower values of $\langle v_x^2 \rangle$ for secondary ions from PS may be indicative of a lower local temperature (energy density) or shorter lifetime before neutralisation of the ion tracks in this material. As the primary ions deposit roughly the same amount of energy in both polymers, the differences in the width of the velocity distributions, obtained for the ions ejected from PVDF and PS targets, should be related to the specific radiation chemistry induced in each polymer. The energy released in the breaking and/or formation of new chemical bonds in the ion track (fast nonequilibrium reactions) may add to the energy deposited directly by the primary ions.

The relatively lower values and the absence of any dependence of $\langle v_x \rangle$ and $\langle E_x \rangle$ on the chemical composition for negative ions from both PS and PVDF suggests that these ions are ejected at later times, after the track has neutralised, and “cooled” considerably. This is in accordance with the fact that prior to neutralisation the infratrack is positively charged. However we cannot eliminate the possibility that the low mass negative ions are formed at times comparable to the time scale of positive ion formation, but preferentially from regions outside the positively charged infratrack.

4. Conclusion

The radial velocity distributions of low mass secondary ions ejected from polymeric targets depend on the chemical composition of the ions. The behaviour of the $\langle v_x \rangle$ indicates that a non-random momentum transfer is also involved in the sputtering of the low mass species. The connection between mean radial energies and the degree of hydrogenation of ejected ions reflects the deposited energy density at the point of ion formation. Hydrocarbon ions with a higher degree of hydrogenation are formed in an outer track region with lower energy density, and at a later moment on the time scale of the energy transfer processes. Our results demonstrate that chemical events in the track (bond breaking and bond rearrangement) are not spatially homogeneous, but depend on the locus of the event, relative to the trajectory of the MeV ion.

Acknowledgements

This work has been supported by the Swedish Natural Sciences Research Council (NFR), the Ångström and Cluster Consortia, and the Wallenberg Foundation. One of us (R.M.P.) acknowledges the National Research Council of Brazil (CNPq) for a fellowship.

References

- [1] R. Fleischer, P. Price and R. Walker, *Nuclear Tracks in Solids* (University of California Press, Los Angeles, 1975).
- [2] B.E. Fischer and R. Spohr, *Rev. Mod. Phys.* 55 (1983) 907.
- [3] *Kinetics of Inhomogeneous Processes* (ed. G. Freeman) (Wiley, New York, 1987).
- [4] K. Roessler, *Nucl. Instr. and Meth. B* 65 (1992) 55.
- [5] R.E. Johnson and B.U.R. Sundqvist, *Phys. Today* (March 1992) 28.
- [6] T. Tombrello, *Nucl. Instr. and Meth. B* 2 (1984) 555.
- [7] P. Haff, *Appl. Phys. Lett.* 29 (1976) 443.
- [8] M. Toulemonde, S. Boufard and F. Studer, these Proceedings (7th Int. Conf. on Radiation Effects in Insulators, Nagoya, Japan, 1993) *Nucl. Instr. and Meth. B* 91 (1994) 108.
- [9] B.U.R. Sundqvist, *Int. J. Mass Spectrom. Ion Processes* 126 (1993) 1.
- [10] T. Tombrello, *Int. J. Mass Spectrom. Ion Processes* 126 (1993) 11.
- [11] R.E. Johnson, *Int. J. Mass Spectrom. Ion Proc.* 78 (1987) 357.
- [12] C.T. Reimann, K. Dan. Vidensk. Selsk. Mat. Fys. Medd. 43 (1993) 351.
- [13] W. Ens, B.U.R. Sundqvist, P. Håkansson, A. Hedin and G. Jonsson, *Phys. Rev. B* 39 (1989) 763.
- [14] Moshhammer, R. Matthäus, K. Wien and G. Bolbach, in: *Ion Formation from Organic Solids (IFOS V)*, eds. A. Hedin, B.U.R. Sundqvist and A. Benninghoven (Wiley, 1990) p. 17.
- [15] R.E. Johnson, B.U.R. Sundqvist, A. Hedin and D. Fenyö, *Phys. Rev. B* 40 (1989) 49; D. Fenyö and R.E. Johnson, *Phys. Rev. B* 46 (1992) 5090.
- [16] I. Bitensky and E.S. Parilis, *Nucl. Instr. and Meth. B* 21 (1987) 26.
- [17] D. Fenyö, A. Hedin, P. Håkansson and B.U.R. Sundqvist, *Int. J. Mass. Spectrom. Ion Proc.* 100 (1990) 63.
- [18] G. Brinkmalm, P. Håkansson, J. Kjellberg, P. Demirev, B.U.R. Sundqvist and W. Ens, *Int. J. Mass Spectrom. Ion Proc.* 114 (1992) 183.
- [19] G. Brinkmalm, P. Demirev, D. Fenyö, P. Håkansson, J. Kopniczky and B.U.R. Sundqvist, *Phys. Rev. B* 47 (1993) 7560.
- [20] T. Tombrello, *Nucl. Instr. and Meth. B* 24/25 (1987) 517.
- [21] H. Danigel and R. Macfarlane, *Int. J. Mass. Spectrom. Ion Phys.* 39 (1981) 157.
- [22] E.J. Kobetich and R. Katz, *Phys. Rev.* 170 (1968) 391.
- [23] W. Brandt and R.H. Ritchie, in R.D. Cooper and R.D. Wood (eds.), *Radiation Biology* (USEC Technical Inf. Center, Oak Ridge, 1974) p. 20.